COMPANY & PROJECT INFORMATION

Company:	SibTech, Inc. 115 Commerce Drive Brookfield, CT 06804
Principal Investigator:	Joseph M. Backer, Ph.D.
Project Title:	Development of Cu-64 labeled EGF for In Vivo PET Imaging of EGFR Expression
Topic 51/a1.	Radiopharmaceutical Development for Radiotracer Diagnosis and Targeted Molecular Therapy
Grant Award Number:	DE-FG02-07ER84905

Proprietary Data Legend N/A

A. IDENTIFICATION AND SIGNIFICANCE OF THE PROBLEM, AND TECHNICAL APPROACH

The overall goal of this project is development of a targeted radiotracer for PET imaging of the receptors for epidermal growth factor (EGFR) in cancer patients. The significance and the impact of such radiotracer is determined by the crucial role that EGFR plays in many cancers and by rapid entrance into the clinic of new drugs that target this receptor (Baselga & Arteaga, 2005). Since only 10-25% of patients respond to these drugs, their rational use requires information on EGFR prevalence to enable 1) patient segmentation, 2) rapid monitoring of responses to therapy, and 3) development of new personalized treatment regimens. Currently, EGFR prevalence is evaluated by immunohistochemical analysis of tissue biopsies, which proved to be rather inefficient in predicting of treatment outcome (Scagliotti, et al., 2004; Chung et al., 2005; Bell et al., 2005). Thus, EGFR imaging with targeted PET radiotracer holds the promise to satisfy unmet clinical needs.

In considering technical approach to development of such radiotracers we decided that using EGF, a natural ligand for EGFR, as a targeting vector might be particularly advantageous. First, EGF binds to EGFR with high affinity and is internalized via receptor-mediated endocytosis, providing for intracellular accumulation of radionuclide. Second, small size of mature EGF would facilitate tumor penetration. Third, as a human protein, EGF is not expected to be immunogenic. Finally, we have recently engineered and expressed functionally active EGF with an N-terminal tag for site-specific conjugation (Cys-tag), derivatized this protein with fluorescent dye Cy5.5 for near-infrared fluorescent imaging, and established that EGF-based contrast agent is functionally active, images tumors in mouse models and accumulates in tumor cells *in vivo* (Backer et al., 2007). Taken together, these argue in favor of using EGF as a targeting vector. As possible disadvantage of using EGF, we consider concerns about potential physiological effects of EGF-based tracers. Although a definitive answer to these concerns requires extensive experimentation, we expect that injection of small amounts of EGF for diagnostic imaging will cause no adverse effects.

For radiolabeling of Cys-tagged EGF we propose to use ^{64}Cu. This selection is based on the following chemical and logistical advantages. First, there is no need for radiochemical synthesis, because radiolabeling with ^{64}Cu needs only a chelator, which is conjugated to the protein via "cold" chemistry. A functionalized macrocyclic chelator DOTA suitable for conjugation is available commercially. In our experience, site-specific conjugation of DOTA to Cys-tagged protein via a pegylated linker does not affect activity of the protein and favorably modify clearance and biodistribution of the resulting ^{64}Cu radiotracer. Second, radiolabeling of protein-chelator conjugate with ^{64}Cu requires only a short incubation followed by purification on a desalting column, which can be done by the end-user immediately before imaging. Third, reasonably high ^{64}Cu stability ($t_{1/2}$ = 12.7 h) allows imaging several hrs after injection of the tracer, thereby improving signal-to-background ratio due to clearance of free and non-specifically bound tracer. Finally, using a similar strategy (site-specific conjugation of DOTA to Cys-tagged protein via a pegylated linker), we are currently developing ^{64}Cu PET radiotracer for imaging receptors for vascular endothelial growth factor in tumor angiogenesis (Backer et al., 2007). This experience, as well as established collaboration with Dr. F. Blankenberg (Stanford University), are fully translatable to this project.

Guided by the significance of the problem and selected technical approach, in Phase I of this project we propose to prepare EGF-based ^{64}Cu PET radiotracer and validate it in mouse tumor model. Accomplishing specific technical objectives with quantitative milestones will allow us to proceed with clinical development of this radiotracer in Phase II and III of the project.

B. ANTICIPATED PUBLIC BENEFITS

We expect that the end-result of this project will be EGF-based ^{64}Cu PET radiotracer approved for clinical use in cancer patients. Molecular imaging of EGF receptors will be a dramatic step to personalized medicine, because it will provide direct information on the prevalence of the drug target and responses to therapy for individual patients. Considering staggering cost of EGFR-targeted therapeutics and positive response only in 10-25% of patients, advances in patient segmentation and monitoring will benefit patient population and will significantly decrease a healthcare cost for the society. Providing targeted PET radiotracer also makes economic sense, as seen from the following estimations. A current price of a contrast agent for PET imaging is ~$500/imaging and it is a relatively small fraction of the overall cost of PET imaging ($3,000-6,000). It is estimated that by 2010, in excess of 2,000,000 PET scans will be performed per year. If a price of a targeted contrast agent will be within $500-1000 range and only 1% of PET scans will be performed with EGF-based PET ^{64}Cu radiotracer, the market size for this tracer might reach $10-20 millions/year.

C. DEGREE TO WHICH PHASE I HAS DEMONSTRATED TECHNICAL FEASIBILITY

Our initial strategy for Phase I was to site-specifically conjugate DOTA to Cys-tagged EGF via a pegylated linker, validate functional activity of the conjugate *in vitro*, prepare EGF-PEG-DOTA/^{64}Cu tracer, establish its biodistribution, and validate it in a mouse tumor model. The following Technical Objectives were proposed for this strategy:

Technical Objective #1. To synthesize and validate *in vitro* EGF-PEG-DOTA conjugate.

Technical Objective #2. To establish clearance, biodistribution, and stability of EGF-based PET ^{64}Cu radiotracer.

Technical Objective #3. To evaluate PET tumor imaging with EGF-based ^{64}Cu radiotracer in mouse tumor models.

In the course of Phase I, we discovered that Cys-tagged proteins can be directly radiolabeled with [^{99m}Tc]pertechnate via a simple and effective procedure (Levashova et al., 2008). Since [^{99m}Tc]pertechnate is approved for clinical use, this finding presented new opportunities for rapid development of EGF/^{99m}Tc and dEGF/^{99m}Tc SPECT tracers. We therefore extended our experiments and included two additional Technical Objectives:

Technical Objective #4. To establish biodistribution of EGF-based SPECT ^{99m}Tc radiotracer.

Technical Objective #5. To evaluate SPECT tumor imaging with EGF-based ^{99m}Tc radiotracer in mouse tumor models.

We will briefly describe the key results obtained for each Technical Objective, and also other relevant results obtained in the course of this project.

Technical Objective #1. To synthesize and validate *in vitro* EGF-PEG-DOTA conjugate.

Cys-tagged EGF and dEGF. To make site-specifically radiolabeled tracers, we use EGF expressed with N-terminal Cys-tag (Fig. 2), 15-aa fusion tag containing a cysteine residue (C4) for site-specific conjugation of various payloads (described in Backer et al., 2007; Cys-tag is reviewed in Backer et al., 2008). Since proper EGFR activity requires dimerization and interaction with two EGF molecules, we considered a possibility that it might be difficult to accommodate two EGF-PEG-DOTA conjugates in such complex. To circumvent this potential problem we engineered a head-to-tail EGF dimer (dEGF) with one Cys-tag (Fig. 2). EGF and dEGF were expressed in *E.coli*, recovered from inclusion bodies, refolded in red-ox buffer containing glutathione, and purified via ion-exchange chromatography (Backer et al., 2007). As other Cys-tagged proteins refolded in red-ox buffer, EGF and dEGF proteins are recovered with C4-thiol group in Cys-tag "protected" in a form of a mixed disulfide with glutathione.

Figure 2. EGF and dEGF. Single or doubled copy of human EGF was cloned in-frame with N-terminal Cys-tag (Backer et al., 2007, 2008). Both proteins were expressed in *E.coli*, refolded into functionally active conformations in red-ox buffers and purified via ion-exchange chromatography.

Conjugate synthesis. PEG-DOTA was conjugated to EGF and to dEGF through the following two-step procedure (Fig. 3a).

Step 1. Activated DOTA is prepared by derivatization of *p*-NH_2-Bn-DOTA (2-(4-Aminobenzyl)-1,4,7,10-tetraazacyclododecane-1,4,7,10-tetraacetic acid) (Macrocyclics, Dallas, TX) with 5 kDa NHS-PEG-MAL, polyethylenglycol (PEG) with amino-reactive NHS group on the one end and thiol-reactive maleimide on the other end of each PEG molecule (NOF America, Terrytown, NY). Activation is performed at 2:1 molar ratio of DOTA to PEG in a buffer containing 15 mM NaOAc, 50 mM Na_2CO_3, 115 mM NaCl, pH 8.0. Reaction is stopped by addition of 1 M Tris HCl pH 8.0 to a final concentration of 100 mM, and incubated for 30 min to hydrolyze unreacted NHS. DOTA-PEG-Mal is stored at -70 ^{o}C in small aliquots.

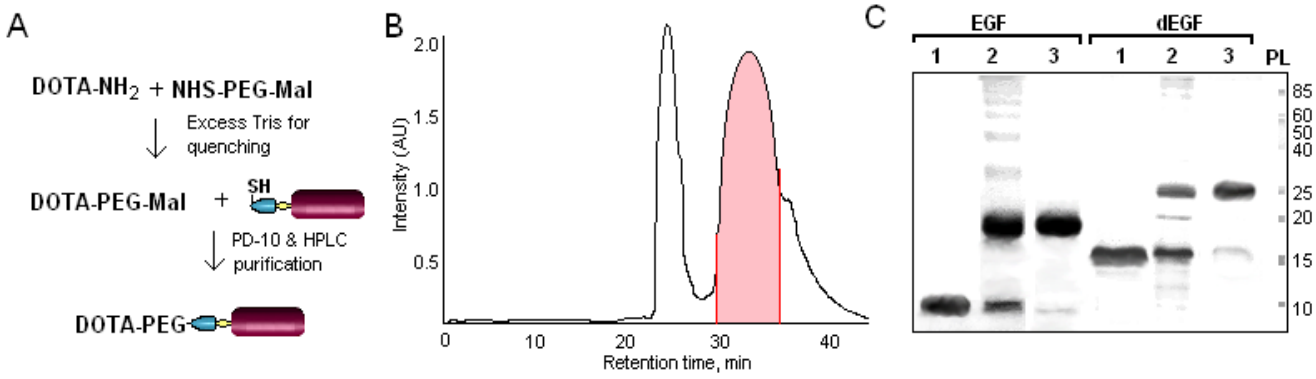

Figure 3. Conjugation DOTA via 5-kDa PEG to EGF and dEGF. A, Flow-chart of synthesis. **B**, Separation of unmodified (40-50%) and over-modified (<10%) EGF by RP-HPLC. Second peak (shown in pink) was collected; buffer-exchanged on PD-10 column, and concentrated to concentration ready for radionuclide loading (1-2 mg/ml). **C,** samples of unmodified proteins (lanes 1), modification reaction mixtures (lanes 2) and RP-HPLC-purified products (lanes 3) were analyzed by reducing SDS-PAGE on 20% gels. PL, protein ladder (BioRad). Molecular weights are indicated in kDa.

Step 2. "Deprotected" EGF (or dEGF) is freshly prepared by incubating EGF with equimolar amount of DTT for 30 min at room temperature, in order to release C4-thiol group from mixed disulfide with glutathione (Backer et al., 2007). DOTA-PEG-Mal conjugate is then added to deprotected protein at the Mal-to-protein ratio of 2:1 and incubated for 1 h at room temperature. The reaction mixture is passed through PD-10 and then fractionated on C4 RP-HPLC, which provides for good separation of unmodified protein and EGF-PEG or dEGF-PEG-DOTA conjugates (Fig. 3b, for EGF). RP-HPLC purification is followed by solvent exchange on PD10 into buffer containing 0.1 M NaOAc pH 5.5. Final preparations are obtained by concentration of purified conjugates via reverse dialysis using Aquacide III powder (Calbiochem) and stored at -70 ^{o}C in small aliquots. As judged by SDS-PAGE, the final preparations contained less then 5% of unmodified protein (Fig. 3c, lanes #3 for EGF and dEGF).

Conjugate activity. Functional activities of EGF-based conjugates are tested in two cell culture based assays. In a short-term assay (10 min), conjugates are tested for the ability to bind to EGFR and induce its tyrosine phosphorylation. In this assay EGF-PEG-DOTA and dEGF-PEG-DOTA displayed similar dose-dependences as parental proteins (Fig. 4a).

In a long-term competition assay (3 days), conjugates are tested for their ability to protect EGFR-positive cells from EGF-based cytotoxin. We reasoned that in this assay binding of EGF-based construct to EGFR reaches equilibrium and eliminates any kinetic effects that might affect binding in a short-term assay. We found that in this assay both EGF-PEG-DOTA and dEGF-PEG-DOTA displayed activity very similar to that of parental proteins (Fig. 4b).

Since loading DOTA chelator with radionuclides takes place at elevated temperature, we also tested how it might affect its functional activity. We found that incubation of EGF-PEG-DOTA conjugates in radiolabeling buffer at 95 ^{o}C for 30 min does not decrease its functional activity (Fig. 4b).

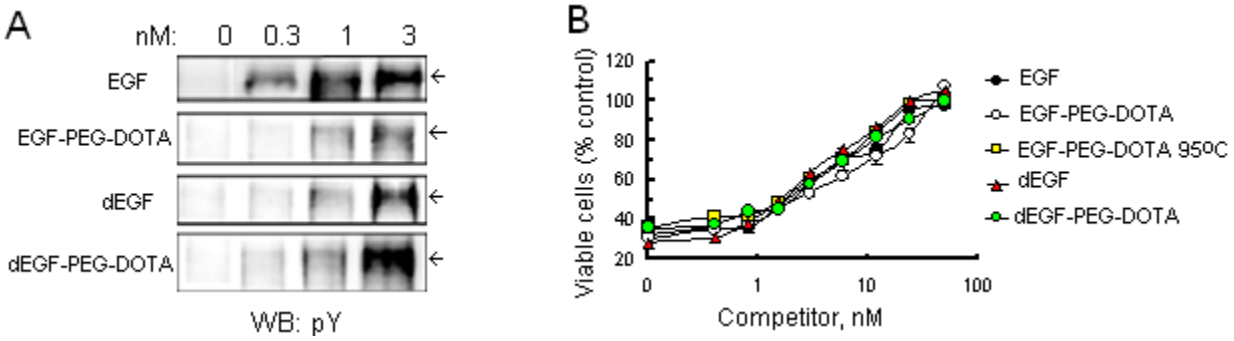

Figure 4. EGF- and dEGF-based conjugates are functionally active. **A,** induction of EGFR tyrosine autophosphorylation in rat F98/EGFR glioma cells expressing 2x10^{6} EGFR/cell. Arrows indicate positions of EGFR. **B,** competition with EGF-toxin fusion protein for binding to EGFR on human breast cancer cells MDA231. Both assays were done as described elsewhere for VEGF/VEGFR-2 binding (Backer et al., 2007).

Radiolabeling of conjugates with ^{64}Cu. The ^{64}Cu radiolabeling protocol was initially developed for scVEGF-PEG-DOTA conjugates (Backer et al., 2007) and it was further optimized as described in details elsewhere (Backer et al., 2008). Briefly, the current protocol is as follows:

1. Transfer 3 mCi ^{64}Cu to 1.5-ml eppendorf tube and adjust pH to 5.3-5.5 with 4 μL 0.3 *M* NaAc, pH 5.5. Check pH by spotting ~0.3 μL on indicator paper. Important note: do not use alkaline solution for pH adjustment as Cu ions will form insoluble hydroxides.
2. Add 4 μL DMSO (or 10 μL for dEGF-PEG-DOTA) and 20 μg of conjugate; check out pH again, it must be in a range 5.0-5.5. The final DMSO concentration must be ~20 % for EGF-PEG-DOTA and ~30% for dEGF-PEG-DOTA.
3. Incubate for 60 min at 55 ^{o}C. Add EDTA to a 1 m*M* final concentration to chelate free ^{64}Cu.
4. Equilibrate PD-10 column with 5 column volumes of PBS.
5. For removal of unreacted ^{64}Cu, load the reaction mixture on equilibrated PD-10 column and elute with PBS.
6. This procedure usually results in incorporation of ~75 μCi of ^{64}Cu per μg of dEGF-PEG-DOTA and ~125 μCi of ^{64}Cu per μg of EGF-PEG-DOTA.

Summary for Technical Objective #1. Functionally active EGF-PEG-DOTA and dEGF-PEG-DOTA are synthesized, protocols for functional testing and radiolabeling are developed. Technical objectives are achieved.

Technical Objective #2. To establish clearance, biodistribution, and stability of EGF-based PET ^{64}Cu radiotracer.

Mouse tumor model. Two mouse models were used in these experiments, 1) F98/EGFR rat glioma (~10^6 EGFR/cell), grown subcutaneously, and 2) luciferase-expressing MDA231luc human breast carcinoma (~$2x10^5$ EGFR/cell), grown orthotopically. 4.5 mln F98/EGFR cells/mouse were injected subcutaneously on the back of 5-6 week old female SCID/NCr (BALB/c background) mice (Charles River Laboratories, Wilmington, MA). 3 mln MDA231luc cells/mouse were injected into the left axillary fat pad of SCID/NCr (BALB/c background) mice. The protocols for all animal studies were approved by the Stanford University Institutional Animal Care and Use Committee and by University of Connecticut Health Center Animal Care and Use Committee

Biodistribution. For biodistribution and imaging studies, 95 μCi of either EGF-PEG-DOTA/^{64}Cu or dEGF-PEG-DOTA/^{64}Cu were intravenously injected into mice (n=4) 9 days after tumor cell implantation. An early time point, when tumors were just palpable (3-5 mm) was selected in order to establish if EGF-based tracers are suitable for early tumor detection. Mice were imaged at 3-4 hours post-injection, and then sacrificed at 22 hours post-injection for biodistribution studies. For biodistribution, blood was collected, organs were harvested, weighed, and counted in a gamma counter with the exception of carcass, which was placed in a glove and counted and normalized to a full dose of injected activity in a dosimetric calibrator. Results were expressed as both % injected dose (ID) and % ID per gram. Accounting for natural decay of ^{64}Cu ($t_{1/2}$=12.7 h) was incorporated into calculations. The data are presented in Fig. 5 as %ID/g and compared with several protein-based ^{64}Cu PET tracers in Table 1.

The major uptake organs, were liver, kidney, and spleen. In all organs, the uptake of the dEGF-based tracer was >3-fold lower than for EGF-based tracer. The tumor uptake in F98/EGFR and MDA231luc tumors was, respectively, 1% and 1.7 %ID/g for EGF-based tracer and 0.3 and 0.3 %ID/g for dEGF-based tracer. Thus, unfortunately, the lower uptake of dEGF-based tracer was observed not only in major organs, but also in tumors. Interestingly, both tracers, the uptake in F98/EGFR tumors was somewhat lower than in MDA231luc, despite the

fact that the latter cells express ~5-fold less EGFR in tissue culture. We found this result very instructive, since it indicates that only functional in vivo tests can provide meaningful information about receptor activity in vivo.

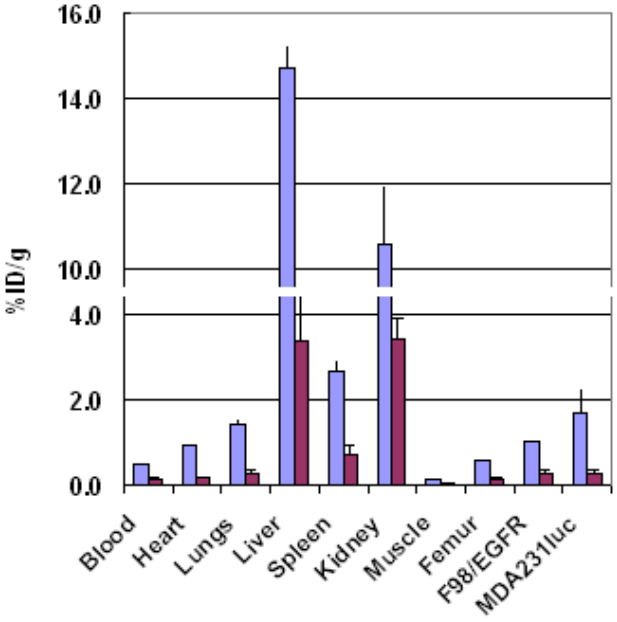

Figure 5. Biodistribution of EGF-PEG-DOTA/^{64}Cu (blue) and dEGF-PEG-DOTA/^{64}Cu (red). Data for major organs are averaged for all tumor-bearing mice. Tumor uptake is averaged for specific tumors. 95 μCi per mouse of EGF/Tc (0.75 μg) or dEGF/Tc (1.25 μg) (n=4 for every tracer) was injected via the tail. Tissue samples were taken at 22 hrs after injection and counted in a gamma counter along with three samples of standard activity (1/100 of injected dose). Results were calculated as the average of the percentage of injected dose per gram (%ID /g) of tissue ± one standard deviation of the mean.

It should be pointed out that at 22-hour post-injection, the uptake in both tumors was still 5-10 times higher that in muscle tissue, providing excellent opportunity for imaging.

Table 1. Major organ uptake (%ID/g) for protein-based ^{64}Cu PET tracers.

	ChCE7F (antibody)	Ch14.18 (antibody)	Single-chainVEGF	VEGF	EGF	dEGF
	Grunberg et al., 2005	Voss et al., 2007	Backer et al. 2007	Cai et al. 2006	Phase I results	
kidney	16	12	60	20	11	3.4
liver	11	7	8	12	15	3.4
spleen	5	6	3	4	2.6	0.7

Stability and clearance. Stability of Cu/DOTA complexes is well-established and is characterized by logKa of ~22 (Smith, 2004). Clearance of EGF-based tracers is described in Technical Objective #4.

Summary for Technical Objective #2. Technical objectives are achieved. Biodistribution of EGF-PEG-DOTA/^{64}Cu and dEGF-PEG-DOTA/^{64}Cu is characterized. Uptake of EGF-based tracer in major organs and tumor is comparable to that that reported for antibody/^{64}Cu tracers.

Technical Objective #3. To evaluate PET tumor imaging with EGF-based ^{64}Cu radiotracer in mouse tumor models.

Our goal in this Technical Objective was to establish feasibility of imaging with EGF-based tracers. In these experiments we used the same tumor models, described in Technical Objective #2. Mice with very small tumors (2-5 mm) were imaged 3-4 hours post-injection. Tumor presence was validated by bioluminescent imaging after intraperitoneal luciferine injection, as described elsewhere (Backer et al., 2007). A typical set of PET images obtained with EGF-PET-DOTA/^{64}Cu and dEGF-PET-DOTA/^{64}Cu in MDA231luc tumor-bearing mice is shown in Fig. 6. The key finding is that tumors (white arrowheads) as small as few millimeters can be detected with both tracers. Similar results were obtained with subcutaneous F98/EGFR tumors.

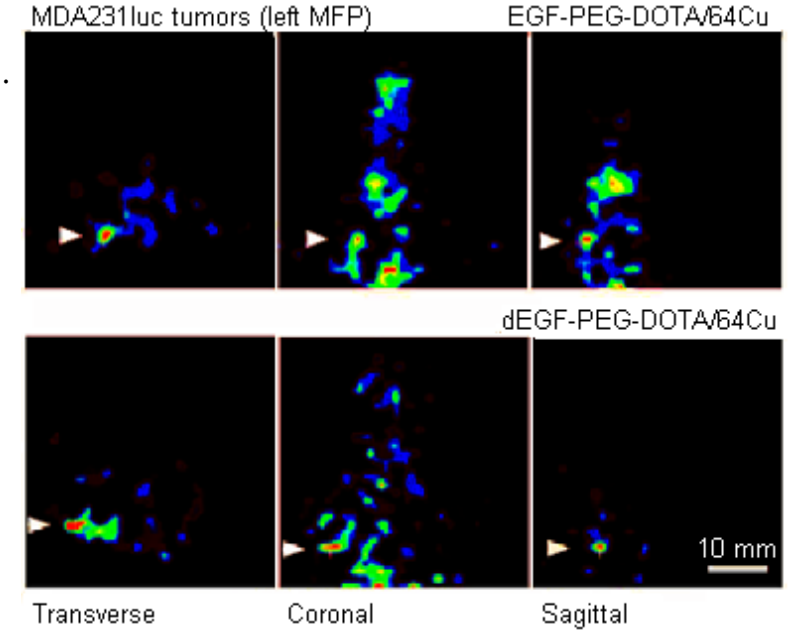

Figure 6. PET imaging Representative transverse, coronal, and sagittal tomographic slices through the left mouse mammary fat pad tumor taken after 2-3 hrs after injection of 95 μCi of EGF-PEG-DOTA/ ^{64}Cu (upper raw) or dEGF-PET-DOTA/^{64}Cu (lower raw). White arrowheads mark the left mammary fat pad tumor.

Two additional tasks were planned for this part of the project. One task was to develop a tracer based on inactivated EGF-PEG-DOTA. Based on our experience with other growth factors, we expected to make inactivated EGF tracers by excessive biotinylation of amino groups. This approach did not work with EGF-based tracers, because biotinylated EGF retained full functional activity. We are now exploring a possibility of development of inactivated tracers based on mutant EGF, which does not bind to the receptor.

The other task was to use siRNA to alter EGFR expression. We decided against using this approach because recent findings indicated that siRNA can alter cell physiology through Toll-like receptor mediated mechanism(s), rather than via expected specific mechanisms (Kleinman et al., 2008). This would complicate interpretation of imaging data and, if pursued, would take us away from the focus on development of the tracers.

Summary for Technical Objective #3. The main task of this technical objective is achieved. We established that EGF- and dEGF-based PET tracers can be used for imaging of very small (3-5 mm) tumors. The auxiliary task was not undertaken for scientific reasons.

Technical Objective #4. To establish biodistribution of EGF-based SPECT ^{99m}Tc radiotracer.

As described in the **Section A. Identification and Significance of the Problem**, in the course of the work on this project we discovered that thiol group in Cys-tag can be directly radiolabeled with [^{99m}Tc]pertechnate, yielding stable and efficient SPECT tracers (Levashova et al., 2008; Backer et al., 2008). We therefore extended our project to establish feasibility of developing EGF-based tracer for SPECT imaging. EGF and dEGF were directly radiolabeled with [^{99m}Tc]pertechnate and the resulting EGF/Tc and dEGF/Tc tracers were explored as imaging agents.

We found that these tracers bind to F98/EGFR cells with expected Kd and N (Fig. 7A), as judged by Scatchard's analysis (Fig. 7A for EGF), are stable in plasma at 37 ^{o}C (see, Fig 7A, for dEGF/Tc) and cleared rapidly from circulation (see, Fig. 7B for dEGF/Tc).

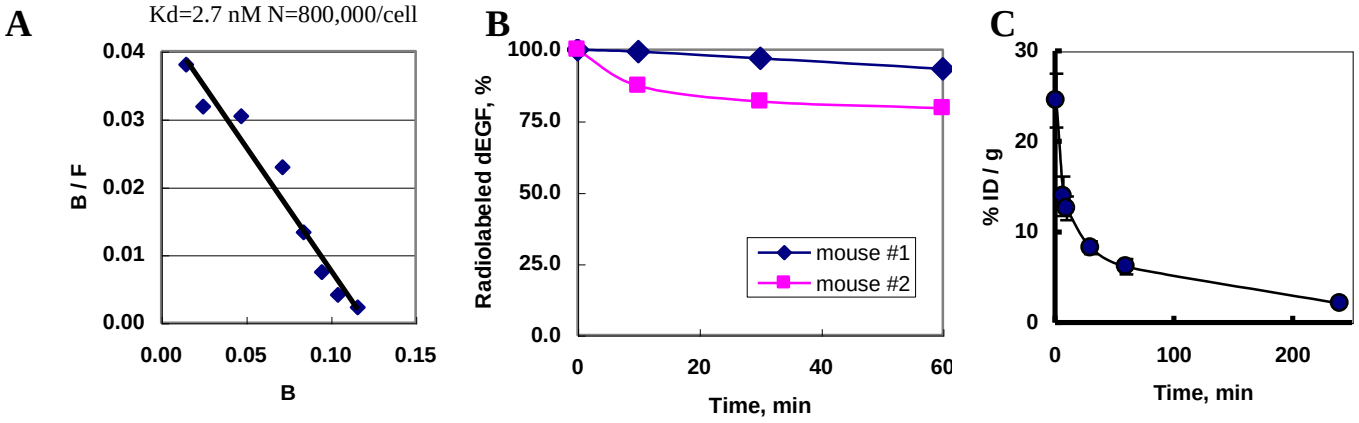

Figure 7. Binding, stability and clearance of EGF/Tc and dEGF/Tc tracers. A, Scatchard's analysis was undertaken with F98/EGFR cells, using protocol described elsewhere (Backer et al., 2007, Levashova et al., 2008). Non-specific binding was determined upon addition of 200-fold excess of cold EGF. **B**, For stability experiments two Balb/c mice were injected i.v. with a tracer (55 µCi/0.25 µg per mouse) and sacrificed 2 min later. Blood was collected and clarified by centrifugation. Plasma samples were incubated at 37 ^{o}C. After 0, 10, 30, and 60 min of incubation, 1-µL plasma aliquots were analyzed by ITLC to determine the protein-bound radioactivity. **C**, For clearance experiments 55 µCi of tracer/mouse (n=4) was injected via the tail vein and serial ~50-µL blood samples were taken via supraorbital sinus at various time points after injection and counted in a gamma counter along with three samples of standard activity (1/100 of injected dose). Results were calculated as the average of the percentage of injected dose per gram (%ID / g) of blood sample ± one STD of the mean.

Biodistribution experiments were performed on MDA231luc tumor-bearing mice with well-formed tumors at 25-day post implantation. Biodistribution data in %ID/g for both EGF/Tc and dEGF/Tc are shown in Fig. 8, and comparison with other proteins in Table 2. We found that dEGF/Tc uptake was higher in kidney and liver, but lower in small and large bowel. Interestingly, uptake in tumor was higher for dEGF/Tc tracer and there were no significant difference between the edge and the center of the tumor.

Table 2. Major organ uptake (%ID/g) for protein-based ^{99m}Tc tracers.

	Antibody fragment	Annexin V	scVEGF/HYNIC	scVEGF	EGF	dEGF

	Berndorff et al. 2006	Verbeke et al. 2003	Backer et al. 2007	Levashova et al. 2008	Phase I	
kidney	21.8	38	120	50	28	47
liver	2.5	24	6	6	15	22

Judging by reasonably similar biodistribution for EGF and dEGF-based tracers, the selection of one of these proteins for further development can be based on opportunities for co-development of PET and SPECT tracers. Since EGF-based PET tracer had higher tumor uptake, we selected EGF for further development.

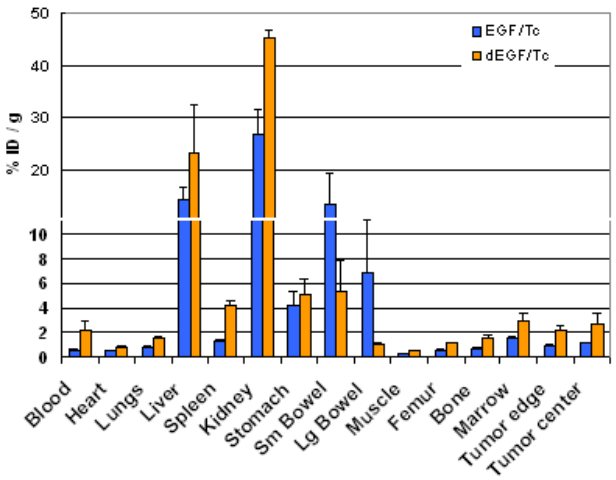

Figure 8. Biodistribution for EGF-based SPECT tracers. 3.1 mCi/10 μg per mouse of EGF/Tc or 0.81 mCi/13 μg per mouse of dEGF/Tc (n=4) was injected via the tail. Tissue samples taken 3 hrs after injection were counted in a gamma counter along with three samples of standard activity (1/100 of injected dose). Results were calculated as the average of the percentage of injected dose per gram (%ID /g) of tissue ± one standard deviation of the mean.

Summary for Technical Objective #4. Technical objectives are achieved. Biodistribution of EGF/^{99m}Tc and dEGF/^{99m}Tc is characterized. Uptake of EGF-based tracers in major organs is comparable to that that reported for other protein-based ^{99m}Tc tracers.

Technical Objective #5. To evaluate SPECT tumor imaging with EGF-based ^{99m}Tc radiotracer in mouse tumor models.

SPECT tracers were tested in two tumor models: orthotopic MDA231luc breast carcinoma and spontaneous mouse lung carcinoma that arise in bi-transgenic mice (FVBN original strain carrying *myc* or *ras* transgenes regulated by a tetracycline-inducible lung-specific promoter. In both models, tracers readily accumulated in tumors (Fig. 9).

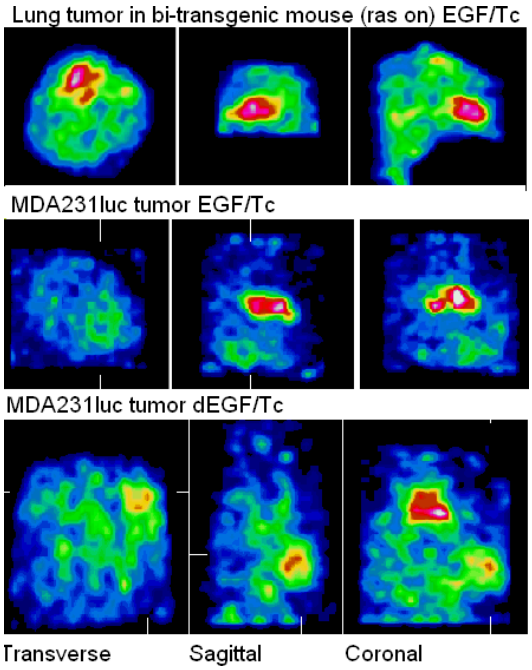

Figure 9. SPECT imaging with EGF/^{99m}Tc. 3.3 mCi/10μg of EGF/Tc or dEGF/Tc per mouse was injected via tail vein. SPECT images were obtained one hour after injection with the following parameters; 360º rotation, 64 steps, 30 seconds per step, 0.5 mm pinhole aperture, a 64 x 64 image matrix and a 3.4 cm FOV using a small animal SPECT imaging gamma camera. Representative transverse, sagittal, and frontal images are shown. **Upper row**, spontaneous lung tumor in bi-transgenic mouse with ras-oncogene expression, EGF/Tc tracer; **Middle row**, orthotopic MDA231luc tumor, EGF/Tc tracer; **Lower row,** orthotopic MDA231luc tumor, dEGF/Tc tracer.

To further explore distribution of tracer, after imaging with EGF-based ^{99m}Tc tracers, we have selected two EGF/Tc-injected mice with MDA231luc tumors, harvested tumors, prepared cryosections, and undertook autoradiography of the sections. Cryosections prepared from contralateral muscle were used as control. As shown in Fig. 10A, radioactivity was significantly higher in tumor cryosections, as compared with muscle cryosections.

In a similar experiment, we selected a bi-transgenic mouse in which SPECT with dEGF/^{99m}Tc-detected tumor only in the left lung, harvested and cryosection both lungs, and undertook autoradiography of cryosections. As shown in Fig. 10B, radioactivity was significantly higher in left lung cryosections, as compare with the right lung.

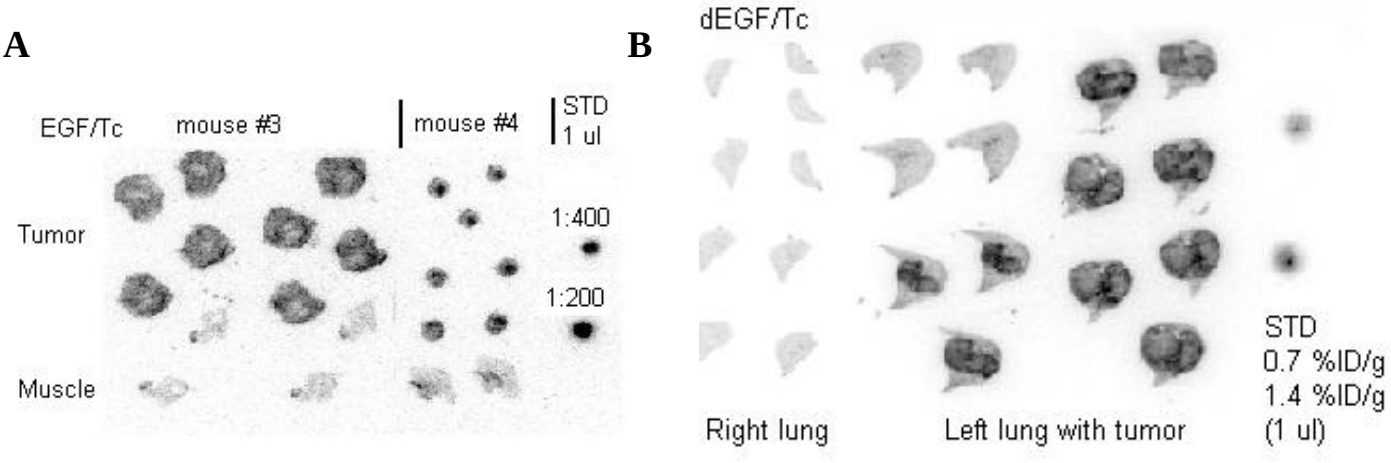

Figure. 10. **Autoradiographs of tumors after imaging with EGF-based ^{99m}Tc tracers.** **A.** SCID mice with orthotopic MDA231luc tumors (25 days after cell injection) have been i.v. injected with 3.1 mCi/10 μg per mouse of EGF/Tc or 0.81 mCi/13 μg of dEGF/Tc. In 4-5 hrs, after SPECT acquisition has been done, the mice have been sacrificed, tumors and pectoralis muscle from the healthy chest side were snap-frozen, cryosectioned (60-μm thickness), and exposed to a phosphor storage screen for 16 hr. The phosphor screen images were read out with a laser digitizer at a resolution of 50 μm per pixel. **B**. Right (healthy) and left (tumor-invaded) lungs of myc-on bi-transgenic mouse

Summary for Technical Objective #5. Technical objective is achieved. EGF/^{99m}Tc and dEGF/^{99m}Tc works as SPECT tracers in two mouse models, with the former providing better biodistribution.

D. REFERENCES

Backer M. V., et al. Molecular imaging of VEGF receptors in angiogenic vasculature with single-chain VEGF driven probes. Nature Med, 13:504-509, 2007.

Backer, M. V., et al. (2008) Cysteine-Containing Fusion Tag for Site-Specific Conjugation of Therapeutic and Imaging Agents to Targeting Proteins. In:. L Otvos, L., Ed. Methods in Molecular Medicine, Peptide-Based Drug Design. The Humana Press Inc., Totowa, New Jersey (In press)

Baselga J, Arteaga CL. Critical update and emerging trends in epidermal growth factor receptor targeting in cancer. J Clin Oncol 23:2445–59, 2005.

Berndorff D., et al. Imaging of Tumor Angiogenesis Using 99mTc-Labeled Human Recombinant Anti-ED-B Fibronectin Antibody Fragments. J Nucl Med. 47:1707-16, 2006.

Bonomi P. D., Buckingham L., and Coon J. Selecting patients for treatment with epidermal growth factor tyrosine kinase inhibitors. Clin Cancer Res. 13(15 Pt 2):s4606-12, 2007.

Cai W., et al. PET of Vascular Endothelial Growth Factor Receptor Expression J Nucl Med. 47:2048-56, 2006.

Chung KY, et al. Cetuximab shows activity in colorectal cancer patients with tumors that do not express the epidermal growth factor receptor by immunohistochemistry. J Clin Oncol 23:1803–10, 2005.

Grunberg J., et al. In vivo evaluation of 177Lu- and 67/64Cu-labeled recombinant fragments of antibody chCE7 for radioimmunotherapy and PET imaging of L1-CAM-positive tumors. Clin Cancer Res. 11:5112-20, 2005.

Hann C. L. and Brahmer J. R. Who should receive epidermal growth factor receptor inhibitors for non-small cell lung cancer and when? Curr Treat Opt Oncol. 8:28-37, 2007.

Johns T. G., et al. The Efficacy of Epidermal Growth Factor Receptor–Specific Antibodies against Glioma Xenografts Is Influenced by Receptor Levels, Activation Status, and Heterodimerization. Clin Cancer Res. 13:1911-25, 2007.

LaCroix, KJ. et al. Receiver operating characteristic evaluation of iterative reconstruction with attenuation correction in 99mTc-sestamibi myocardial SPECT images. J Nuc. Med. 41: 502-513, 2000.

Lalush, DS. & Tsui BM. Performance of ordered-subset reconstruction algorithms under conditions of extreme attenuation and truncation in myocardial SPECT. J Nucl Med. 41: 737-744, 2000.

Lalush, DS. et al. Fast maximum entropy approximation in SPECT using the RBI-MAP algorithm. IEEE Trans Med Imaging 19, 286-294 (2000).

Levashova, Z., Backer, M., Backer, J. M., Blankenberg, F. G. (2008) Direct site-specific labeling of the Cys-tag moiety in scVEGF with Technetium 99m. Bioconjugate Chem. (accepted).

Scagliotti GV, et al. The biology of epidermal growth factor receptor in lung cancer. Clin Cancer Res. 10:4227–32s, 2004.

Smith S. V., Molecular imaging with copper-64. J Inorg Biochem 98:1874–1901, 2004.

Vallis KA, Reilly RM, Chen P, et al. A phase I study of 99mTc-hR3 (DiaCIM), a humanized immunoconjugate directed towards the epidermal growth factor receptor. Nucl Med Commun. 23:1155–64, 2002.

Velikyan I. Sundberg AL. Lindhe O. et al. Preparation and evaluation of (68)Ga-DOTA-hEGF for visualization of EGFR expression in malignant tumors. J Nucl Med**.** 46(11):1881-8, 2005.

Verbeke K. et al. Optimization of the preparation of 99mTc-labeled Hynic-derivatized Annexin V for human use. Nucl Med Biol. 30:771-8, 2003.

Voss S. D., et al. Positron emission tomography (PET) imaging of neuroblastoma and melanoma with 64Cu-SarAr immunoconjugates. Proc Natl Acad Sci USA 104:17489-93, 2007.